J. Phys. B: At. Mol. Opt. Phys. **41** (2008) 205204 (8pp) doi:10.1088/0953-4075/41/20/205204

Polarization effects in electron collisions with Li_2: application of the molecular *R*-matrix method with pseudostates

M Tarana[1] **and J Tennyson**[2]

[1] Institute of Theoretical Physics, Charles University in Prague, V Holešovičkách 2, Prague, Czech Republic
[2] Department of Physics and Astronomy, University College London, Gower Street, London WC1E 6BT, UK

E-mail: tarana@mbox.troja.mff.cuni.cz

Received 17 June 2008, in final form 26 August 2008
Published 6 October 2008
Online at stacks.iop.org/JPhysB/41/205204

Abstract

Li_2 has a huge polarizability and a huge elastic cross section for collisions with low-energy electrons. The recently developed molecular *R*-matrix with pseudostates (MRMPS) method is applied to electron collisions with Li_2 at energies below 5 eV. The calculations, which are shown to be stable with respect to the choice of pseudostate basis, demonstrate the power of the MRMPS method for representing target polarizabilities and polarization effects in general. A previously identified low-lying $^2\Pi_u$ shape resonance is found at about 0.05 eV and several other low-lying resonances and resonance-like features are identified. Cross sections for elastic and electronically inelastic electron collisions are calculated and compared with previous studies.

(Some figures in this article are in colour only in the electronic version)

1. Introduction

Ab initio treatments of electron–molecule scattering have now become fairly routine for small and medium sized molecules at low energy, i.e. energies below the ionization threshold of the molecule. The hardest part of such calculations is to completely converge the polarization potential part of the calculation (Gil *et al* 1994), which is particularly important at low collision energies. The lithium dimer provides a benchmark system for this problem since it is the molecule with the largest known static polarizability. As a direct consequence of this it also has the largest low-energy, elastic, electron–molecule cross section so far observed for a neutral, nonpolar molecule (Miller *et al* 1982). The Li_2 molecule thus forms a theoretical benchmark against which the reliability of *ab initio* electron–molecule scattering procedures can be tested.

Recently, Gorfinkiel and Tennyson (2004, 2005) have developed a molecular *R*-matrix with pseudostates (MRMPS) method for treating electron collisions at intermediate energies. Although this was not their prime objective, Gorfinkiel and Tennyson found that their MRMPS calculations gave excellent values for the target polarizability and resulted in an improved representation of the polarization potential. Subsequent calculations on resonances in electron impact detachment from C_2^- (Halmová and Tennyson 2008, Halmová *et al* 2008) showed how polarization effects modelled using the MRMPS method could tackle problems not amenable to more standard treatments. The huge polarizability of Li_2 provides a very stringent test of the ability of the MRMPS to model such polarization effects and it is this that we test here.

Total cross sections for electron–Li_2 scattering have been measured by Miller *et al* (1982) and dissociative attachment measurements were performed by McGeoch and Schlier (1986). Theoretical treatments of the scattering problem have been performed by Padial (1985) and Gil *et al* (1993). These workers found a rich structure of Li_2^- resonances at low collision energies but found that their calculations were very sensitive to the precise treatment of polarization effects particularly at energies below 1 eV.

2. Method

The *R*-matrix method is based on dividing coordinate space into two regions using a spherical boundary centred on the centre-of-mass of the target molecule (Burke and Berrington 1993, Burke and Tennyson 2005). The radius of the boundary, a, is chosen so that the inner region contains all the electronic charge cloud of the target molecular states included in the calculation. The best value for a raises issues for Li_2 since the large internuclear separation (calculations here are presented for the equilibrium bondlength of 5.05 a_0) and the diffuse nature of the target wavefunction require the use of a larger than usual inner region. Hereafter for tests with a up to 22 a_0, a radius of 18 a_0 was chosen.

The accuracy of this method is strongly dependent on the representation of the problem in the inner region (Tennyson 1996) where it is necessary to consider all short-range interactions between the N target electrons and the scattering one. In standard, low-energy calculations, the wavefunction for an (N+1)-electron system in the inner region is given by the expansion

$$\psi_k^{N+1} = \mathcal{A}\sum_{ij} a_{ijk}\Phi_i(\mathbf{x}_1\cdots\mathbf{x}_N)u_{ij}(\mathbf{x}_{N+1}) + \sum_i b_{ik}\chi_i(\mathbf{x}_1\cdots\mathbf{x}_{N+1}), \quad (1)$$

where k represents the kth solution of the inner region Hamiltonian, $\mathcal{A}$ is the antisymmetrization operator, $\mathbf{x}_i$ are the spatial and spin coordinates of electron i, u_{ij} are continuum orbitals (COs) which represent the scattering electron (Tennyson and Morgan 1999), a_{ijk} and b_{ik} are variational coefficients, Φ_i is the wavefunction of the ith target state and χ_i are L^2 functions constructed from the target occupied and virtual molecular orbitals. These functions represent electron correlation and polarization effects. In the first sum, the configuration state functions are constrained to give the correct (target) space and spin symmetry for the first N electrons as well as the correct total, $(N+1)$-electron space–spin symmetry. The target wavefunctions are expanded as linear combinations of the configurations ϕ_k

$$\Phi_i(\mathbf{x}_1\cdots\mathbf{x}_N) = \sum_k c_{ik}\phi_k(\mathbf{x}_1\cdots\mathbf{x}_N), \quad (2)$$

where the c_{ik} coefficients are determined by diagonalizing the Hamiltonian of the molecular target.

The central idea of the MRMPS method is the augmentation of the close-coupling expansion (1) with extra pseudo-state 'target' wavefunctions Φ_i which are represented using an extra basis of pseudo-continuum orbitals (PCOs). Unlike the usual target wavefunctions, these pseudo-states are not approximations to true eigenstates of the target, but are used to represent a discretized version of both the electronic continuum and the high-lying target states not included in the expansion. These pseudo-states are obtained by diagonalizing the target electronic Hamiltonian expressed in an appropriate basis of configurations.

The addition of an extra basis means that care must be taken with orthogonalization of the final orbital set. This is done by first Schmidt orthogonalizing the PCO to the target molecular orbitals (MOs) and then deleting those transformed PCOs with the eigenvalues of the overlap matrix less than a deletion threshold $\delta_{\rm thr}^{\rm PC}$. This procedure is then repeated for the COs which are orthogonalized to the target MOs plus PCOs and those COs whose eigenvalues of the overlap matrix are less than $\delta_{\rm thr}^{\rm CO}$ are deleted. Further discussion on this can be found in the original references (Gorfinkiel and Tennyson 2004, 2005).

Calculations were performed using Gaussian type orbitals (GTOs) and the UK polyatomic *R*-matrix code (Morgan *et al* 1997). In the polyatomic suite target orbitals, COs and MRMPS PCOs are all represented by a linear combination of GTOs. The highest symmetry available in the polyatomic code is D_{2h} which is a subgroup of the true $D_{\infty h}$ symmetry of Li_2. All calculations presented here were performed in D_{2h} symmetry.

3. Calculations

3.1. Target representation

The Li_2 target was represented using Hartree–Fock molecular orbitals (MOs) using a cc-pVTZ GTO basis set from which we removed the most diffuse p-orbital in order to confine the molecule inside a sphere with $a = 18$ a_0. The removal of this GTO is compensated by the PCOs used in the MRMPS calculations (see below). As all the usual GTO bases of the lithium atom contain at least one diffuse Gaussian, use of smaller primary basis set would not lead to more compact MOs without loss of quality of the ground-state description. On the other hand, use of a larger primary target basis set raises issues for the optimization of the COs. Therefore, use of the cc-pVTZ GTO basis with the most diffuse orbital removed is a good compromise between the compactness of the MOs and quality of the target representation (see below). We note that as the majority of our target MOs were retained in the calculations and used to represent the target wavefunction, our calculation should therefore not be sensitive to the details of the choice of target orbitals, as has been found previously (Gil *et al* 1993).

Calculations using three different sets of N-particle states in the close-coupling expansion were carried out. In the first of them no PCOs were used, the COs were orthogonalized on the MOs only. Two other calculations were performed using different PCO bases. This allows us to understand the effect of polarization as well as to control the stability of our calculations with respect to small changes of the PCO basis.

For the PCOs we followed Gorfinkiel and Tennyson (2004, 2005) and used their even-tempered bases rescaled for $a = 18$ a_0. The first of them with $\alpha_0 = 0.0525, \beta = 1.3$ (denoted as PC-1 in the following) was obtained by multiplying $\alpha_0^{\rm orig} = 0.17$ by a factor of $\gamma = (10/18)^2$. The second basis with $\alpha_0 = 0.0463, \beta = 1.3$ (denoted as PC-2 in the following) was adopted in the same way from the original basis as $\gamma \times 0.15$. In all cases we restricted the PCO basis to $l \leqslant 3$ (10s, 10p, 6d, 5f) in order to keep the calculation tractable. To avoid problems with linear dependence of the COs, the two highest virtual MOs from the irreducible representation

Table 1. The number of molecular orbitals (MOs), pseudo-continuum orbitals (PCOs) and continuum orbitals (COs) in the irreducible representations of the D_{2h} point group. The numbers in the second and third lines without brackets correspond to the PC-1 basis ($\alpha_0 = 0.0525$), while the numbers in the brackets correspond to the PC-2 basis ($\alpha_0 = 0.0463$).

	A_g	B_{2u}	B_{3u}	B_{1g}	B_{1u}	B_{2g}	B_{3g}	A_u
MOs	10	6	6	3	8	6	6	2
PCOs	9	7	7	4 (3)	3	2	2	1
COs	16 (15)	15	15	5	15	5	5	5

A_g were removed as well as the four highest MOs from B_{1u} and the highest MO from A_u. The numbers of MOs used in the calculations are listed in table 1. To avoid the linear dependence with the PCOs a deletion threshold in the orthogonalization between the PCOs and target MOs was set to $\delta_{\rm thr}^{\rm PC} = 5 \times 10^{-4}$, as a result not all the orthogonalized PCOs were used in the scattering calculation. The numbers of used PCOs in all the irreducible representations are listed in table 1.

The Li_2 target states were represented using a complete active space (CAS) valence configuration interaction (CI) wavefunction. In these calculations we kept the two lowest MOs doubly occupied. Using the notation for the irreducible representations of D_{2h} this gives a CAS of the form

$$(1a_g, 1b_{1u})^4$$
$$(2-10a_g, 1-6b_{2u}, 1-6b_{3u}, 1-3b_{1g}, 2-8b_{1u}, 1-6b_{2g}, 1-6b_{3g}, 1-2a_u)^2. \quad (3)$$

For the MRMPS calculations a second, additional set of target configurations was generated using the following prescription and added to configurations (3):

$$(1a_g, 1b_{1u})^4 2a_g^1$$
$$(11-19a_g, 7-13b_{2u}, 7-13b_{3u}, 4-7b_{1g}, 9-11b_{1u}, 7-8b_{2g}, 7-8b_{3g}, 3a_u)^1 \quad (4)$$

for PC-1; for PC-2 the highest b_{1g} PCO is absent. Table 2 shows vertical excitation energies for the low electronic states of Li_2 calculated using these models. Our results both with and without PCOs are consistent with, but slightly higher than, accurate *ab initio* calculation of Hanrath (2005) which appears to be due to neglect of correlation effects associated with the core electrons. The corresponding distribution of calculated CI physical and pseudostates for different bases is plotted in figure 1. It shows that both calculations including PCOs produce some pseudostates with energy above the ionization threshold which is marked.

To check how well our target models represent the target ground-state polarizability of Li_2 we calculate the parallel ($\alpha_\parallel$) and perpendicular ($\alpha_\perp$) components of the polarizability tensor from the transition dipole moments using the following sum-over-states formulae,

$$\alpha_\parallel = \frac{1}{2}\sum_{i>1}\frac{|\langle\Phi_1|z|\Phi_i\rangle|^2}{\Delta E_i}, \qquad \alpha_\perp = \frac{1}{2}\sum_{i>1}\frac{|\langle\Phi_1|x|\Phi_i\rangle|^2}{\Delta E_i}, \quad (5)$$

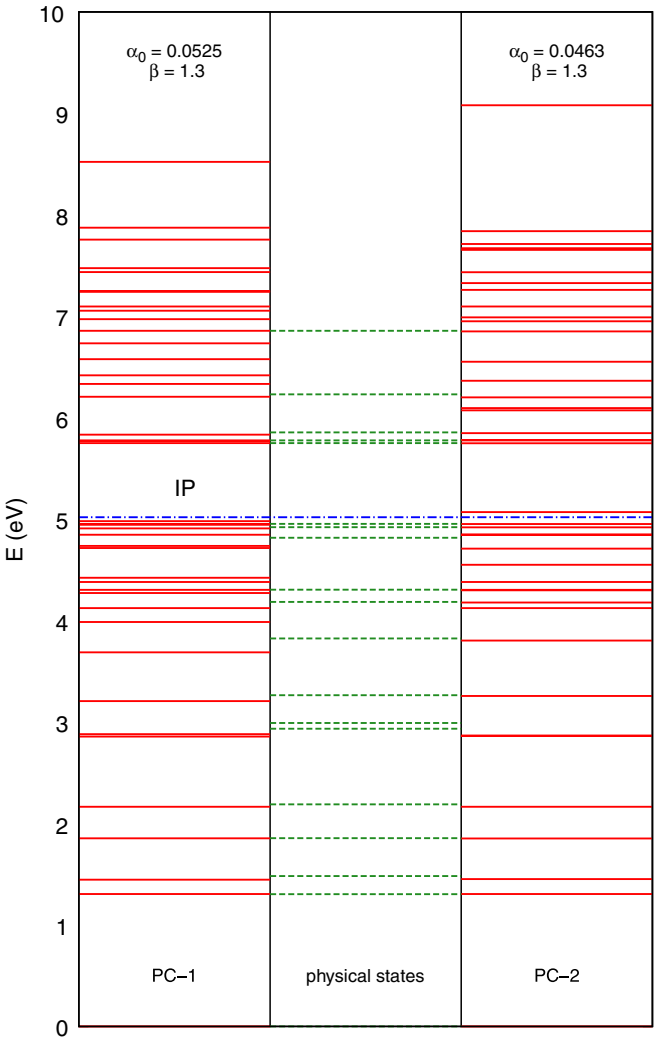

Figure 1. Calculated distribution of pseudostates for PC-1 and PC-2 bases (left and right columns) and physical target state distribution (middle column). All energies are relative to $X^1\Sigma_g^+$. The line with label IP indicates the ionization threshold taken from Boldyrev *et al* (1993).

where Φ_1 and Φ_i are wavefunctions of the target ground state and ith electronic state (2), ΔE_i is the corresponding ith excitation energy. By construction this sum runs only over states in the inner region; however the MRMPS method is designed to allow for the contribution of the continuum. Provided the state for which the polarizability is being computed is contained within the inner region, this method should recover all contributions to the polarizability.

Our tests are summarized in table 3. Target calculations without pseudostates show that only very few states are needed to reach convergence. While the parallel component ($\alpha_\parallel$) converges to within high accuracy using three lowest $^1\Sigma_u^+$ states, the perpendicular component ($\alpha_\perp$) converges to underestimated value as can be seen in table 3.

Calculation using the same set of states including the PC-1 basis shows improvement of $\alpha_\perp$. As table 3 shows, use of five pseudostates in the corresponding irreducible representations improves the results to better than 90% agreement with previously published *ab initio* calculations (Mérawa and Rérat

Table 2. Ground state (in hartree) and vertical excitation energies (in eV) for the basis without PCOs, for bases PC-1 ($\alpha_0 = 0.0525$, $\beta = 1.3$), PC-2 ($\alpha_0 = 0.0463$, $\beta = 1.3$) and Hanrath (Hanrath 2005).

Electronic state		Vertical excitation			
$D_{\infty h}$	D_{2h}	No PCOs	PC-1	PC-2	Hanrath
$X^1\Sigma_g^+$	^1A_g	−14.9027	−14.9027	−14.9027	−14.9134
$1^3\Sigma_u^+$	$^3B_{1u}$	1.305	1.305	1.305	1.231
$1^3\Pi_u$	$^3B_{2u} + {}^3B_{3u}$	1.483	1.447	1.454	1.370
$1^1\Sigma_u^+$	$^1B_{1u}$	1.856	1.854	1.854	1.778
$1^3\Sigma_g^+$	^3A_g	2.190	2.166	2.166	2.122
$1^1\Sigma_g^+$	^1A_g	2.936	2.882	2.868	2.783
$1^1\Pi_u$	$^1B_{2u} + {}^1B_{3u}$	2.992	2.858	2.864	2.798
$1^1\Pi_g$	$^1B_{2g} + {}^1B_{3g}$	3.266	3.208	3.259	2.998
$1^3\Pi_g$	$^3B_{2g} + {}^3B_{3g}$	3.825	3.689	3.806	3.130

Table 3. Static dipole polarizability (au) of the Li_2 ground state using PC-1, PC-2 and basis without PCOs. The second and third columns give number of states used in the sum-over-states formula contributing to the corresponding component.

	Number of states		Polarizability	
Basis set	$^1\Sigma_u^+$	$^1\Pi_u$	$\alpha_\parallel$	$\alpha_\perp$
Without PCOs	3	1	308	127
Without PCOs	141	126	309	132
PC-1	3	1	306	143
PC-1	4	5	307	146
PC-1	144	133	308	147
PC-2	4	5	306	145
Accurate *ab initio* value (Mérawa and Rérat 2001)			303	160

2001). For all the models tested the main contribution to the polarizability is due to the lowest state. These results show the advantage of pseudostates in our next calculations: with quite a small number of pseudostates we are able to represent the low target excited states correctly as well as the target ground-state polarizability better than with a larger number of target states without any PC basis. Tests showed that using all PCOs gives results close to the *ab initio* values of Mérawa and Rérat (2001). We decided not to use these additional PCOs in our scattering calculations to avoid problems with linear dependence of the COs.

Here it is worth making two points about the polarization potential in the scattering calculation. The first is that the polarizabilities, as shown in table 3, do not appear in this form in the actual calculation. They are represented in the outer region by coupling to (often closed) channels by the transition dipole moments which are included in the multipole expansion. In the inner region the polarizability is similarly represented by coupling between target states but the CI formulation of the problem automatically includes exchange and other effects which make the polarization impossible to represent as a single, energy-independent potential. Secondly, as shown to be important below, this formulation also allows for the polarization of excited states of the target. Given that these states are increasingly diffuse, their polarizabilities are even larger than the already very large polarizability of the ground state. Tests showed that our MRMPS values for these polarizabilities are in good agreement with previously calculated values (Mérawa and Rérat 2001). The effect of this is clearly seen in the difference between our MRMPS and non-MRMPS calculations reported below at energies above the lowest threshold for electronic excitation.

3.2. Scattering calculation

The larger R-matrix radius used in our calculations requires larger continuum basis sets than used in standard calculations with smaller R-matrix spheres. The corresponding single centre GTO exponents are listed in table 4. This basis set was optimized using the program GTOBAS (Faure *et al* 2002). Tests of the validity of this basis set using calculations in a potential-free R-matrix (Tarana and Horáček 2007) and static exchange calculations for the elastic electron collision with Li_2 in different symmetries showed that it represents the scattering continuum correctly for scattering energies $E \lesssim 5$ eV i.e. below the threshold to ionization (Boldyrev *et al* 1993). We restrict our study to energies below this threshold.

A continuum basis up to $l = 3$ (10s, 9p, 10d, 9f) is used in most of our calculations; g-orbitals were also optimized but their role showed to be negligible at energies below 1 eV. However, as discussed below, they become more important at higher energies but their use leads to a significant increase in the cost of the calculation. The deletion threshold in the orthogonalization procedure for the COs was set to $\delta_{\rm thr}^{\rm CO} = 2 \times 10^{-5}$ (Morgan *et al* 1997). Using this rather high value we optimized 81 (80) COs in the calculation without PC bases and in the calculation with PC-1 (PC-2), see table 1.

Scattering models using the PC-1 and PC-2 bases can be compared with calculations not using pseudostates. The MRMPS (non-RMPS) calculation included all states up to

Table 4. The exponents of the uncontracted continuum GTO basis set used in the calculations optimized for the *R*-matrix sphere with radius $a = 18$ a_0.

$l = 0$	$l = 1$	$l = 2$	$l = 3$	$l = 4$
0.0 396 299	0.0 397 592	0.0 409 729	0.0 425 261	0.0 368 324
0.0 301 133	0.0 311 803	0.0 326 507	0.0 342 543	0.0 295 860
0.0 230 215	0.0 246 211	0.0 262 072	0.0 277 975	0.0 239 172
0.0 175 737	0.0 194 282	0.0 210 283	0.0 225 556	0.0 193 086
0.0 133 473	0.0 152 654	0.0 168 071	0.0 182 352	0.0 155 100
0.0 100 611	0.0 119 135	0.0 133 474	0.0 146 512	0.0 123 578
0.0 075 100	0.0 092 122	0.0 105 059	0.0 116 696	0.0 097 304
0.0 055 326	0.0 070 341	0.0 081 677	0.0 091 824	0.0 075 149
0.0 039 930	0.0 052 652	0.0 062 261	0.0 070 855	
0.0 023 000		0.0 031 000		

Table 5. Positions and widths of resonances (eV) using the PC-1, PC-2 and basis without PCOs.

Symmetry		Without PCOs		PC-1		PC-2	
$D_{\infty h}$	D_{2h}	Position	Width	Position	Width	Position	Width
$^2\Pi_u$	$^2B_{2u} + {}^2B_{3u}$	0.072	0.054	0.055	0.038	0.055	0.040
$^2\Delta_g$	^2A_g	1.582	0.239	1.514	0.174	1.522	0.176
	$^2B_{1g}$	1.568	0.158	1.506	0.141	1.514	0.142
$^2\Pi_g$	$^2B_{2g} + {}^2B_{3g}$	1.120	0.372	1.036	0.583	1.094	0.704
				2.310	0.329		
				2.944	0.190		
$^2\Delta_u$	$^2B_{1u}$			2.170		2.170	
	^2A_u	2.244	0.613	2.105	0.449		
$^2\Sigma_u^-$	^2A_u			1.576	0.597	1.710	0.514

5.8 eV above the ground state; selected states above this energy were included to ensure (a) minimum of 5 (3) states in each of A_g, B_{1u} (B_{2u}, B_{2g}) symmetries and (b) that in all cases both members of a degenerate pair were included. As a result, our close-coupling expansions corresponding to the PC-1 and PC-2 models include 68 pseudostates and expansion not using PCOs includes 28 target states.

4. Results

4.1. Resonances

Our calculated eigenphase sums show resonance features in several symmetries for all models. Their parameters were determined by fitting to a Breit–Wigner formula (Tennyson and Noble 1984). It should be noted that the large number of electronic excited states in the 2–4 eV range led to a number of resonance-like features whose eigenphases show a sharp rise of less than π which stops upon the opening of a new target state. This sort of behaviour has been observed in previous detailed calculations (Branchett *et al* 1990). Those resonances whose parameters could be successfully characterized in this fashion are summarized in table 5; features lying above 3 eV are not included as our characterization of excited states is less complete at these energies.

In general all resonances are shifted down slightly with the introduction of the pseudostates as would be expected from the improved treatment of polarization effects and, indeed, from the variational nature of the calculations. Sufficient PCOs were included in the calculations so that the positions and widths of the low-lying resonances are stable as indeed they are to changes of PCO basis. None of our calculations showed any pseudoresonance below 2 eV. The lowest lying resonance is a $^2\Pi_u$ shape resonance. Our parameters calculated can be compared with those of Padial (1985) who found a position of 0.00 645 eV and a width of 0.0017 eV. Gil *et al*'s (1993) calculations show this resonance in the elastic cross section near 0.06 eV, although the authors do not give any parameters.

A $^2\Delta_g$ Feshbach resonance was found independently in the ^2A_g and $^2B_{1g}$ irreducible representations of the D_{2h} point group. Fits in both symmetries give similar position and width. Analysis of the ^2A_g and $^2B_{1g}$ eigenphases assigned to particular eigenchannels (not given) showed several clear resonance-like changes of the eigenphases in the energy interval 2–3 eV. These structures are not strongly pronounced in the eigenphase sum and their fitting to a Breit–Wigner formula was unstable, especially for the resonance width.

The richest resonance structure appears in $^2\Pi_g$ symmetry. The lowest resonance in this symmetry is of a Feshbach nature showing a well-pronounced peak in the elastic scattering cross section. Padial (1985) found a 'very broad' $^2\Pi_g$ shape resonance about 1 eV. Our position agrees with this and, somewhat unusually, this resonance gets broader as the polarization potential is improved.

There are two further $^2\Pi_g$ resonances below 3 eV, each appears in the eigenphases assigned to particular eigenchannels. However, they do not lead to rapid change of the eigenphase sum and we were only able to determine the corresponding resonance parameters in the PC-1 basis calculation. In the remaining calculations the corresponding structures in the eigenphases disappear or are too close to

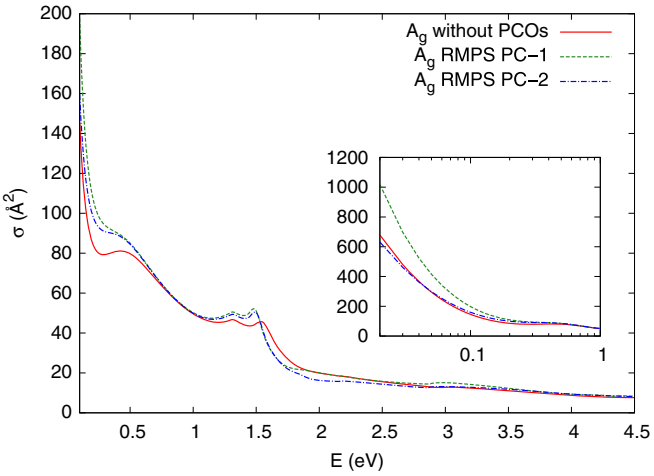

Figure 2. Elastic electron scattering cross section in the ^2A_g symmetry.

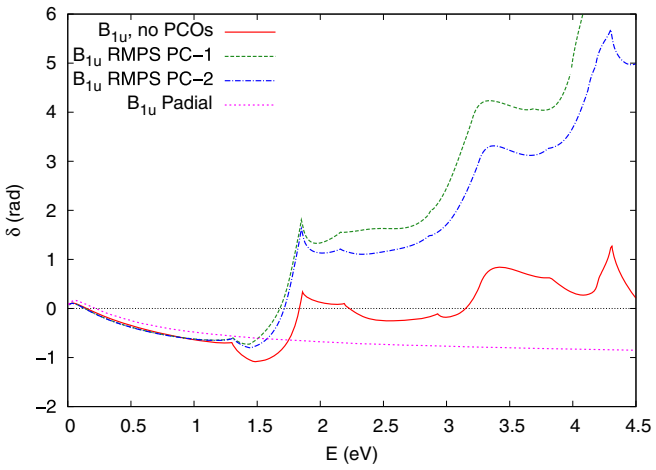

Figure 3. $^2B_{1u}$ symmetry eigenphase sums as a function of model; note that the π has been subtracted from the published values of Padial (1985) to aid comparison.

electronic thresholds to be fitted. It is possible that these resonances are artefacts of the PCO basis.

The presence of the low-lying target states and pseudostates also complicates fitting of resonances in $^2B_{1u}$ symmetry. The corresponding eigenphase sum (figure 3) as well as the elastic scattering cross section (not shown) show a resonance near 1.8 eV. There is no similar structure in ^2A_u eigenphases, indicating that this resonance has $^2\Sigma_u^+$ symmetry in $D_{\infty h}$. The discontinuity in the eigenphases at the $^1\Sigma_u^+$ excitation threshold prevents stable fits of this resonance. In calculations using PCOs we determined the position of another resonance at 2.17 eV, but were unable to find its width due to instability of the fits. The corresponding structure appears in the ^2A_u symmetry calculated, therefore this resonance has $^2\Delta_u$ symmetry. An additional resonance appears in the ^2A_u symmetry at energy 1.576 eV (1.710 eV) using the PC-1 (PC-2) basis set. It is assigned to $^2\Sigma_u^-$ symmetry of the $D_{\infty h}$ point group and does not appear in calculations without pseudostates.

4.2. Cross sections and eigenphases

Our elastic scattering cross sections calculated with pseudostates are, in general, in good agreement with calculations not using PCOs; nevertheless there are points where the polarization plays its role. The ^2A_g symmetry cross section, shown in figure 2, calculated without pseudostates shows a peak around 0.5 eV. This is not a resonance and the corresponding eigenphases are dominated by the s-wave (Tarana *et al* 2008) without any resonance-like features. We did not find any pseudoresonances in the energy region below 2 eV. This peak, which is present at similar energies in previous studies (Tarana *et al* 2008), disappears in the calculations with the PC-1 and PC-2 bases. Its presence is therefore just an artefact of an incomplete treatment of polarization. The exceptionally large ^2A_g cross section at ultra-low energies is due to a virtual state which is present at the Li_2 equilibrium geometry (Gil *et al* 1993, Tarana *et al* 2008). As can be seen in figure 2, the calculation using PC-2 is in good agreement with calculation not using PCOs. The cross section with PC-1 differs almost by a factor of 2 in this energy region. The reason is in the sharp change of the eigenphases close to the zero-energy threshold. At these energies even a very small change in the target basis, leading to a small change in the eigenphases, causes a large change of the cross sections. All our calculated elastic cross sections are in good agreement at energies above 1 eV.

A sharp change in the $^2B_{1u}$ symmetry cross section is also found at very low energies. The presence of a sharp peak in the cross section at zero energy is connected with the large spatial extent of the negative ionic wavefunction which leads to rapid changes of the eigenphases at very low energies. The $^2B_{1u}$ cross sections show a minimum near 0.1 eV due to the eigenphase sum passing through zero, see figure 3.

In general the cross sections and eigenphase sums show very good agreement between all our models below 1 eV. At higher energies cross sections using different PC bases correspond to each other but show pronounced structures corresponding to resonances absent in cross sections computed without PCOs. However above this the eigenphase sums and hence also the cross sections are very sensitive to inclusion of electronically excited states in the calculation. This is illustrated in figure 3 which shows that our results differ radically from the single-state calculations of Padial (1985) at these energies. Figure 3 shows that the eigenphases corresponding to different MRMPS calculations differ more with increasing energy while the elastic cross sections remain very close to each other. This sensitivity is largely due to the behaviour of eigenphases associated with channels coupling to electronically excited states of Li_2. Presumably, this is a reflection of the treatment of polarization in these channels. This behaviour is displayed by all symmetries.

Our total elastic scattering cross sections are given in figure 4 which shows excellent agreement between our calculations. The low-energy behaviour is determined by the large cross section in $^2\Sigma_g^+$ symmetry and by the presence of the resonance in $^2\Pi_u$ symmetry (see table 5). As the figure shows, the slight change of the resonance position and the threshold

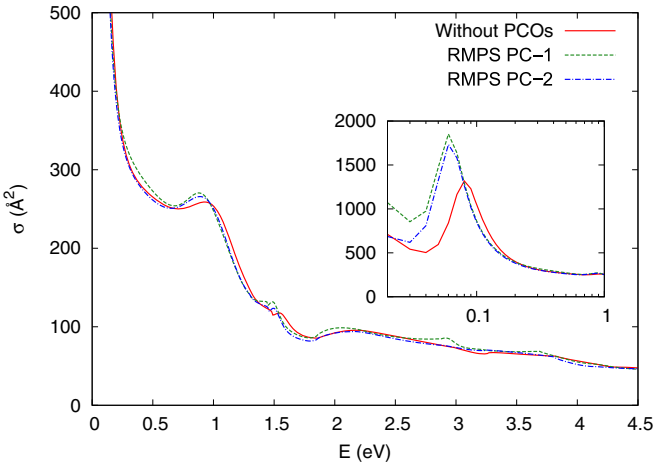

Figure 4. Total elastic electron scattering cross sections.

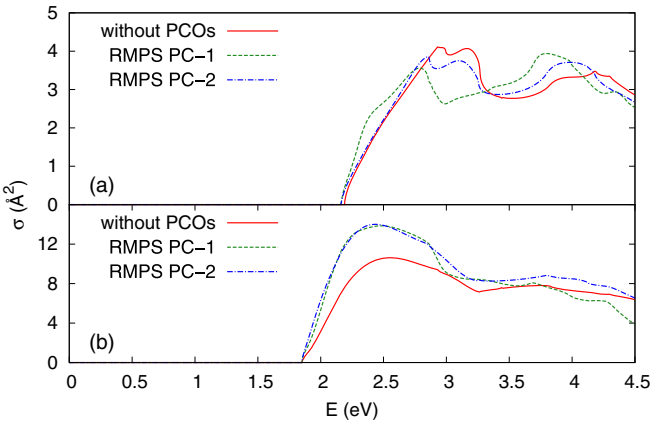

Figure 5. Electron impact electronic excitation cross sections for excitation into the $1^3\Sigma_g^+$ excited state (a) and $1^1\Sigma_u^+$ excited state (b).

behaviour with change of the PCO basis is the dominant factor in the differences between compared results.

Figure 5 shows the integral cross sections for electronic excitation from the ground state to the $1^3\Sigma_g^+$ and $1^1\Sigma_u^+$ states. Although the cross sections calculated using different basis sets differ in detail, the general character of the corresponding cross sections is very similar. Both cross sections are fairly small compared to the corresponding elastic cross section, although the dipole-allowed excitation to the $1^1\Sigma_u^+$ state is larger.

Figure 6 compares our elastic cross sections with previous calculations. Our results, which are for the PC-1 model, are in particularly good agreement with the best model of Gil *et al* (1993) in the 0.1–1 eV energy interval. Gil *et al* (1993) did not consider higher energies while at lower energies their results depend strongly on the target basis set used. While the calculation with averaged natural orbitals shows very good correspondence near the peak assigned to the $^2\Pi_u$ resonance, the cross-section calculated using the ground-state natural orbitals increases rapidly with energy approaching the zero threshold. The difference between our results and Gil *et al*'s (1993) at the low-energy limit might also be caused by the different treatment of the long-range polarization potential.

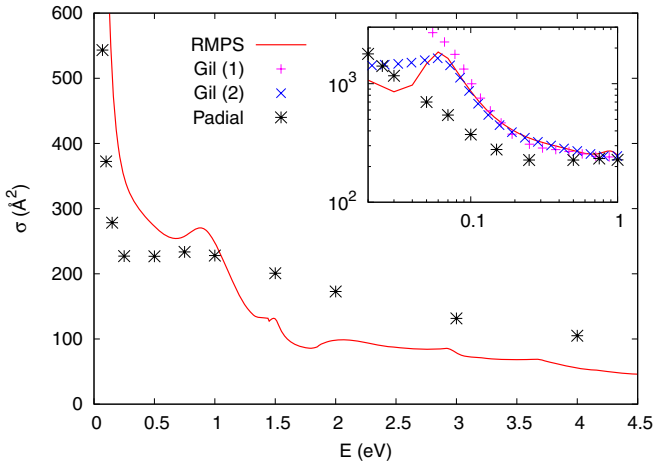

Figure 6. Elastic scattering cross section calculated using the PC-1 basis given by the solid line. Cross sections due to Padial (1985) are given by stars; *Ab initio* elastic cross section due to Gil *et al* (1993) using ground-state (1) and averaged (2) natural orbitals are indicated in the figure.

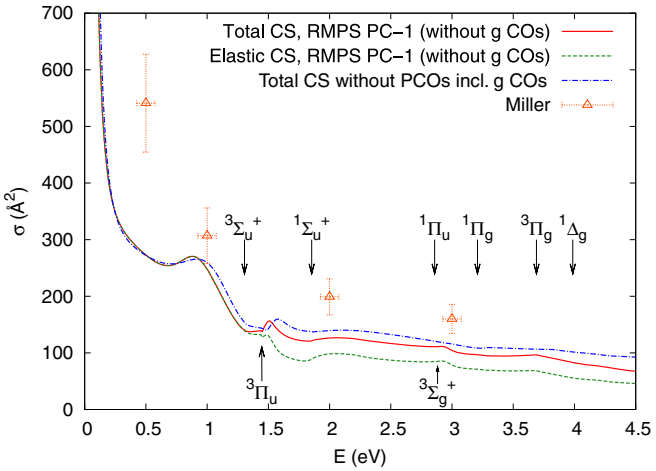

Figure 7. Total (elastic plus electronic excitation) cross section calculated using the PC-1 basis. Experimental data due to Miller *et al* (1982) are given by triangles with errorbars.

Padial (1985) also reported strong dependence of the elastic cross sections on the asymptotic polarization treatment for energies below 1 eV. Figure 6 contains its total cross-section calculated using a model without the cutoff polarization potential. These values are systematically below our results for energies below 1 eV. Padial's (1985) model with a cutoff potential shows a peak close to the $^2\Pi_u$ resonance in better agreement with our calculations, but its position and width were found to change rapidly with the cutoff parameter.

Miller *et al* (1982) measured total rather than just elastic cross sections. Figure 7 compares these measurements with the sum of our MRMPS elastic and electronically inelastic cross sections. The measurements are systematically higher than our results; at higher energies this could be in part due to the truncated set of partial waves used for our COs. However these are very difficult experiments which were performed using a beam of Li_2 at about 1000 K; it is therefore hard to be sure if figure 7 really presents a like-for-like comparison.

5. Conclusions

We report a study of low-energy electron collisions with the Li_2 molecule using the molecular *R*-matrix with pseudostates (MRMPS) method. Using only a few pseudostates we are able to treat the polarizability of this system in more consistent way than previous studies (Padial 1985, Gil *et al* 1993) and represent low-lying target states correctly. We show that our results are stable with respect to small changes of the pseudostate basis. We confirm the presence of a low-energy $^2\Pi_u$ shape resonance found in previous studies (Padial 1985, Gil *et al* 1993) and found several new Feshbach resonances at energies below 3 eV. However it proved difficult to fully characterize these resonances due to the density of low-lying target states.

We present elastic and electronically inelastic scattering cross sections for energies below the Li_2 ionization threshold. This appears to be the first *ab initio* calculation of electron collisions with the Li_2 molecule at energies above 1 eV which includes excited target states and thus allows for electronically inelastic processes.

Acknowledgments

This work is partially supported by the ESF EIPAM—exchange grant 1789, by the grant GAUK 116-10/257718 of the Charles University Prague and by the Center of Theoretical Astrophysics no. LC06014 of the Ministry of Education, Youth and Sports of the Czech Republic.

References

Boldyrev A I, Simons J, von R and Schleyer P 1993 *J. Chem. Phys.* **99** 8793–804
Branchett S E, Tennyson J and Morgan L A 1990 *J. Phys. B: At. Mol. Opt. Phys.* **23** 4625–39
Burke P G and Berrington K A (ed) 1993 *Atomic and Molecular Processes, an R-matrix Approach* (Bristol: Institute of Physics Publishing)
Burke P G and Tennyson J 2005 *Mol. Phys.* **103** 2537–48
Faure A, Gorfinkiel J D, Morgan L A and Tennyson J 2002 *Comput. Phys. Commun.* **144** 224–41
Gil T J, Lengsfield B H, McCurdy C W and Rescigno T N 1994 *Phys. Rev.* A **49** 2551–60
Gil T J, McCurdy C W, Rescigno T N and Lengsfield B H 1993 *Phys. Rev.* A **47** 255–263
Gorfinkiel J D and Tennyson J 2004 *J. Phys. B: At. Mol. Opt. Phys.* **37** L343–50
Gorfinkiel J D and Tennyson J 2005 *J. Phys. B: At. Mol. Opt. Phys.* **38** 1607–22
Halmová G, Gorfinkiel J D and Tennyson J 2008 *J. Phys. B: At. Mol. Opt. Phys.* **41** 155201
Halmová G and Tennyson J 2008 *Phys. Rev. Lett.* **100** 213202
Hanrath M 2005 *J. Chem. Phys.* **123** 084102
McGeoch M W and Schlier R E 1986 *Phys. Rev.* A **33** 1708–17
Mérawa M and Rérat M 2001 *Euro. Phys. J.* D **17** 329
Miller T M, Kasdan A and Bederson B 1982 *Phys. Rev.* A **25** 1777–78
Morgan L A, Gillan C J, Tennyson J and Chen X 1997 *J. Phys. B: At. Mol. Opt. Phys.* **30** 4087–96
Padial N T 1985 *Phys. Rev.* A **32** 1379–1383
Tarana M and Horáček J 2007 *J. Chem. Phys.* **127** 154319
Tarana M, Nestmann B M and Horáček J 2008 at press
Tennyson J 1996 *J. Phys. B: At. Mol. Opt. Phys.* **29** 6185–201
Tennyson J and Morgan L A 1999 *Phil. Trans.* A **357** 1161–73
Tennyson J and Noble C J 1984 *Comput. Phys. Commun.* **33** 421–4